Mechanics of Advanced Materials and Structures, 15:508–513, 2008

ISSN: 1537-6494 print / 1537-6532 online
DOI: 10.1080/15376490802142684

Taylor & Francis
Taylor & Francis Group

Restrictions to the Energy Density in Energetic Models of Carbon Fiber Reinforced Carbon

T.-A. Langhoff and E. Schnack
Institut für Technische Mechanik, Universitaet Karlsruhe (TH), Karlsruhe, Germany

In this contribution an energetic model for multi-phase materials is developed describing the influence of microstructure on different length scales as well as the evolution of phase changes. Restrictions on the energy functional are discussed. In such a non-convex framework, interfacial contributions serve for relaxing the total energy. Such models can be applied to describe the macroscopic material properties of carbon fiber reinforced carbon where phase transitions between regions of different texture of the carbon matrix are observed on a nanoscale as well as columnar microstructures on microscale.

Keywords energetic model, thermodynamics, carbon fiber reinforced carbon, interface phase transformation

1. INTRODUCTION

State-of-the-art composites, e. g., silicon carbide, carbon fiber reinforced carbon (CFC) or polymer/ceramic composites, can be classified as multi-phase materials. Either the phases are composed from different materials (as in the case of silicon carbide) or from different modifications of one material (as in the case of CFC). The number of applications of such materials is actually rapidly increasing: high performance brake systems [1], telescopes for space application based on sintered silicon carbide [2], metal matrix composites such as lightweight composite wires [3], just to name a few. Especially for CFC, the dimensioning with respect to thermomechanical loading is of utmost importance since in almost all applications of CFC, high temperatures are present.

Moreover, using modern experimental set-up for structural characterization, quite rich microstructure can be observed in composites. Aiming to model the macroscopic response of such composites, the microstructure at different length scales has to be taken into account (whose influence even on macroscopic properties is nowadays out of discussion but quantitatively not modelled so for) as well as possible phase transformations between the different phases. In regard to the ever growing number of applications of such composites in a huge number of domains, the need for material models cannot be underestimated. Moreover, developments in applied mathematics and scientific computing additionally favor this aim.

As an example of such a composite we will concentrate on CFC which is most often produced by chemical vapor infiltration where the pyrolytic carbon matrix is deposited around fibers during the long and costly process [4]. Depending on the scale of observation different microstructures can be observed in CFC [5, 6] (see Figure 1). On nanoscale for example, the building blocks of the microstructure are called turbostratic domains and describe regions of a few nm within which the basal planes of carbon possess a common normal vector (see Figure 1c).

This has lead to a new scheme of classification of different phases of carbon depending on the orientation distribution of these normal vectors [8]: one distinguishes between low, medium and high textured phases (see Figure 2) depending on the width of the distribution of the angles of the normal vectors of these basal planes.

The new classification scheme relies on the precise measurement of the so-called orientation angle OA. This angle can be measured using selected area electron diffraction (SAED) which allows the analysis of submicron structures like in carbon fiber reinforced composites instead of the previous scheme based on polarized light microscopy (PLM) [9].

Experimental results for different mechanical properties of the different textures of carbon [7] justify denoting these different textures as different phases. Additionally, around carbon fibers (see Figure 1b), pyrolytic carbon layers with different texture degree's have been detected [6]. The differently textured layers can be considered as phases of pyrolytic carbon [10–12]. Experimental hints for such phase transitions in CFC under high-temperature treatment are reported in [13].

So far hierarchical material models exist for CFC [14] that compute, using an engineering approach, the macroscopic material properties based on a whole hierarchy of length scales and appropriate microstructure. In such models, the different phases of the matrix and the fibers are treated as separate materials with individual mechanical properties. However, only the multi-scale character of the material is taken into account but

Address correspondence to T. A. Langhoff, Institut für Technische Mechanik, Universitaet Karlsruhe, Kaiserstrasse 12, 76128 Karlsruhe. E-mail: langhoff@itm.uni-karlsruhe.de

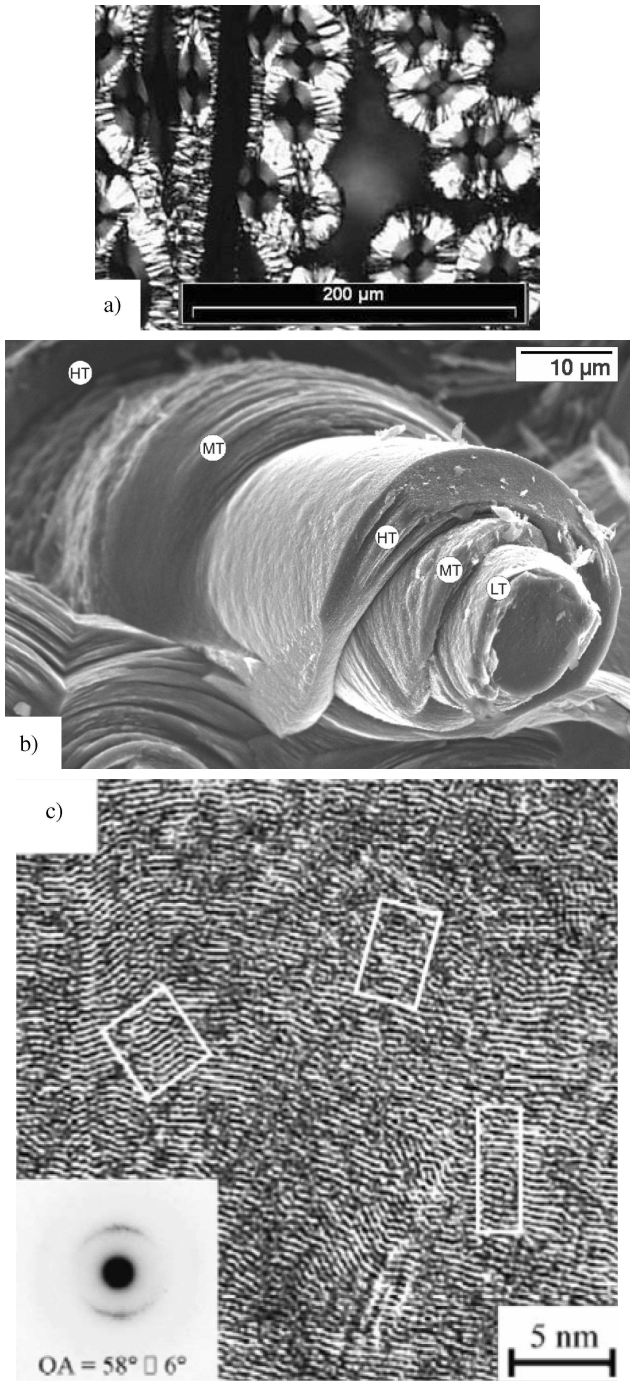

FIG. 1. Microstructures of CFC on different length scales. a) on macroscale [7], b) on microscale [6], c) on nanoscale [5].

phase transitions have not been included. The role of interface energy also is not clarified.

Energetic models have been developed for a wide range of problems in many of which the energy functionals are no longer convex (see, e.g., [15]). The advantage of such energetic models since derivatives do not occur is their applicability to situations where the fields are not smooth (e.g., composites). Instead an energy conservation equation as well as a stability inequality in global form have to be satisfied. For rate independent problems incremental variational formulations have been proposed [16]. A model for phase transformation driven by temperature changes has recently been proposed [17]. Here the crucial assumption is the decoupling of the thermoelastic problem by treating the temperature field as an "applied load" and as a non-constant equilibrium of the heat equation [18]. Moreover, in this approach there is no interface energy specified, but some temperature-independent regularizing contribution to the energy.

In this contribution we start to develop an energetic model for CFC. We aim to describe the macroscopic material response of CFC including the effect of solid-solid phase transitions. The methodology is general allowing a direct generalization to the framework of multi-phase multi-scale materials.

2. THE ENERGETIC MODEL FOR THE NON-ISOTHERMAL CASE

The energetic formulations for rate-independent systems in the isothermal case goes back to Mielke [18]. Key ingredients of such an approach are the functional for the stored energy, ε, and the dissipation distance, $\mathcal{D}$. The main advantage of energetic models is their applicability to situations where derivatives of the fields might not exist at some points and convexity might also not be realized. This is true in many situations where several phases with different material properties coexist within one material: the jumping material parameters destroy the smoothness of solutions and the question of an energy minimum with several phases directly touches the convexity properties.

Energetic formulations consist of a stability inequality as well as an energy conservation equation [19]. An extension to an abstract framework [16] (but still for isothermal situations) no longer relies on the linear structure of the function spaces under consideration and thus is inherently applicable to non-linear material behavior, for example.

To be more precise, we now state the notation and then give the stability inequality and the energy conservation. Note however, that we generalize the formulation for the non-isothermal case. This is necessary in order to describe CFC since the phase transitions are experimentally observed under high-temperature treatment.

We have an open and bounded domain $\Omega \subset \mathbb{R}^3$ with boundary $\Gamma = \partial\Omega$ and the displacement field $\boldsymbol{u} \in W^{1,p}(\Omega, \mathbb{R}^3)$ is unknown. Considering boundary conditions on one part of the boundary,

$$\boldsymbol{u} = \bar{\boldsymbol{u}} \quad \text{on } \Gamma_u \subset \Gamma, \tag{1}$$

we can define the space of admissible displacements

$$\mathcal{F} = \{\boldsymbol{u} \in W^{1,p}(\Omega, \mathbb{R}^3) : \boldsymbol{u} = \bar{\boldsymbol{u}}|_{\Gamma_u}\} \tag{2}$$

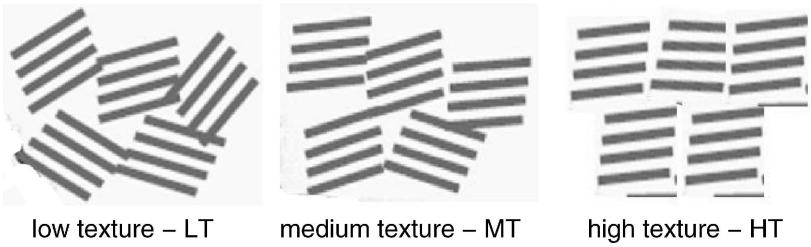

FIG. 2. Definition of different textures using distribution of orientation of normal vectors on turbostratic domains.

Let $\mathcal{P}$ denote the set of phases. To be able to quantify the microstructure throughout the domain Ω we need an indicator to which phase each material point belongs. Consequently, this relation is a piecewise constant relation with values in $\mathcal{P}$. We call

$$\mathcal{S} = \{\hat{\boldsymbol{s}} \in BV(\Omega, \mathbb{R}^3) \cap L^\infty(\Omega, \mathcal{P}) : \hat{\boldsymbol{s}} \quad \text{is piecewise constant}\} \tag{3}$$

the *set of internal states* describing the microstructure of the material within the domain Ω. However, due to phase transformations, such a map can only be valid for a specific instant of time and it is necessary to specify, what phase distribution we have at what time. This is precisely the definition of the *curve of internal states* $s : [0; T] \to \mathcal{S}$: for each time instant $t \in [0; T]$ we have with $s(t) \in \mathcal{S}$ such a distribution, thus nothing other than an internal state $\hat{s}$. Thus, $s(t)[x]$ yields the phase at time instant $t \in [0; T]$ at the material point at $x \in \Omega$. Additionally, we need to consider the absolute temperature θ as a function of time, in order to describe, e.g., high temperature treatment: $\theta : [0, T] \to \mathbb{R}_+$. Focusing on domains with typical dimensions in the micro-range, we assume the temperature to be constant within Ω, thus there is no need to treat a thermal conductivity system. However, temporally changing temperature has a significant effect through the constitutive response of the material by thermoelasticity. In case of thermoelasticity, the typical decomposition of the total strains into the elastic ε^{el} part and the thermal part ε^{th} is used:

$$\varepsilon^{tot} = \varepsilon^{el} + \varepsilon^{th}$$

Based on this notion we can now define the stored energy $\mathcal{E}(t, \boldsymbol{u}, \boldsymbol{s}, \theta)$ for any given tuple $(t, \boldsymbol{u}, \boldsymbol{s}, \theta) \in \mathbb{R}_+ \times \mathcal{F} \times \mathcal{S} \times \mathbb{R}_+$ to be simply the sum of an elastic contribution, $\mathcal{E}_{elast}(t, \boldsymbol{u}, \boldsymbol{s}, \theta)$, a contribution of the interfaces, $\mathcal{E}_{inter}(t, \boldsymbol{u}, \boldsymbol{s}, \theta)$, and an external potential energy, $\mathcal{E}_{ext}(t, \boldsymbol{u}, \theta)$:

$$\mathcal{E}(t, \boldsymbol{u}, \boldsymbol{s}, \theta) = \mathcal{E}_{elast}(t, \boldsymbol{u}, \boldsymbol{s}, \theta) + \mathcal{E}_{inter}(t, \boldsymbol{u}, \boldsymbol{s}, \theta) - \mathcal{E}_{ext}(t, \boldsymbol{u}, \theta) \tag{4}$$

Here, the elastic part is expressed via the elastic energy density W

$$\mathcal{E}_{elast}(t, \boldsymbol{u}, \boldsymbol{s}, \theta) = \int_\Omega W(\boldsymbol{x}, \boldsymbol{Du}(\boldsymbol{x}), \boldsymbol{s}(\boldsymbol{x}), \theta)\, \mathrm{d}\boldsymbol{x} \tag{5}$$

where—as usual in linear elasticity—the strains are given as symmetric gradients of the displacements

$$\boldsymbol{Du} = \frac{1}{2}(\nabla \boldsymbol{u} + (\nabla \boldsymbol{u})^T) \tag{6}$$

and the external energy is given by

$$\mathcal{E}_{ext} = \int_\Omega \boldsymbol{f}(\boldsymbol{x}) \cdot \boldsymbol{u}(\boldsymbol{x})\, \mathrm{d}\boldsymbol{x} + \int_\Gamma \boldsymbol{t}(\boldsymbol{x}) \cdot \boldsymbol{u}(\boldsymbol{x})\, \mathrm{d}\boldsymbol{x}\,, \tag{7}$$

where $\boldsymbol{f}(\boldsymbol{x})$ denotes the density of the volume forces and $\boldsymbol{t}(\boldsymbol{x})$ denotes the tractions on the boundary.

For describing the solid-solid phase transition between states $\boldsymbol{s}_a$ and $\boldsymbol{s}_b$, we use the dissipation distance $\mathcal{D}$, which is given by

$$\mathcal{D}(\boldsymbol{s}_a, \boldsymbol{s}_b, \theta) = \int_\Omega \tilde{\mathcal{D}}(\boldsymbol{s}_a(\boldsymbol{x}), \boldsymbol{s}_b(\boldsymbol{x}), \theta)\, \mathrm{d}\boldsymbol{x} \tag{8}$$

where $\tilde{\mathcal{D}}$ denotes the dissipation metric. For the dissipation distance, we require the triangle inequality:

$$\mathcal{D}(\boldsymbol{s}_1, \boldsymbol{s}_2, \theta) \le \mathcal{D}(\boldsymbol{s}_1, \boldsymbol{s}_3, \theta) + \mathcal{D}(\boldsymbol{s}_3, \boldsymbol{s}_2, \theta) \quad \forall \boldsymbol{s}_i \in \mathcal{S}, i = 1, 2, 3 \tag{9}$$

Now the extension of the energetic formulation by including temperature reads:

Find $(\boldsymbol{u}, \boldsymbol{s}) \in \mathcal{F} \times \mathcal{S}$ such that $\forall t \in [0; T]$

$$\mathcal{E}(t, \boldsymbol{u}(t), \boldsymbol{s}(t), \theta(t)) \le \mathcal{E}(t, \tilde{\boldsymbol{u}}, \tilde{\boldsymbol{s}}, \theta(t)) + \mathcal{D}(\boldsymbol{s}(t), \tilde{\boldsymbol{s}}, \theta(t)) \quad \forall (\tilde{\boldsymbol{u}}, \tilde{\boldsymbol{s}}) \in \mathcal{F} \times \mathcal{S} \tag{10}$$

and

$$\mathcal{E}(t, \boldsymbol{u}(t), \boldsymbol{s}(t), \theta(t)) + \mathcal{E}_{diss}(t, \boldsymbol{s}(t), \theta(t)) = \mathcal{E}(0, \boldsymbol{u}_0, \boldsymbol{s}_0, \theta_0) - \tilde{\mathcal{E}}_{ext}(t, \boldsymbol{u}(t), \theta(t)) \tag{11}$$

Here, the contribution of the external potential energy to the energy conservation (11) is given by

$$\tilde{\mathcal{E}}_{ext} = \int_\Omega \dot{\boldsymbol{f}}(x) \cdot \boldsymbol{u}(x)\,\mathrm{d}\boldsymbol{x} + \int_\Gamma \dot{\boldsymbol{t}}(x) \cdot \boldsymbol{u}(x)\,\mathrm{d}\boldsymbol{x}$$

and the complete dissipated energy during the time interval $[0; t]$ is

$$\mathcal{E}_{diss}(t, \boldsymbol{s}(t), \theta(t)) = \sup \sum_{j=1}^{N} \mathcal{D}(\boldsymbol{s}(t_{j-1}), \boldsymbol{s}(t_j)) \quad \forall N \in \mathbb{N}, \\ \forall \text{ partitions } \{t_j\}$$

For numerical computations, an incremental formulation is useful. We define a partition of the time interval $[0; T]$, such that $0 = t_0 < t_1 < \cdots < t_N = T$ and set $\theta_k := \theta(t_k)$ as well as $y = (\tilde{\boldsymbol{u}}, \tilde{\boldsymbol{s}}) \in \mathcal{Y} := \mathcal{F} \times \mathcal{S}$. Find $\{y_1, \ldots, y_k\}$ such that

$$\mathcal{E}(t_k, y_k, \theta_k) = \inf_{y \in \mathcal{Y}} \{\mathcal{E}(t_k, y, \theta_k) + \mathcal{D}(y_{k-1}, y, \theta_k)\} \qquad (12)$$

Progress in analysis of existence theorems for energetic models can be referred for the isothermal case [16]:

- both the interface energy $\mathcal{E}_{inter}$ and the elastic energy $\mathcal{E}_{elastic}$ have to be sequentially lower semicontinuous,
- the elastic energy density W has to be coercive with respect to the deformation in the second argument
- continuity assumption for external loading (replacing the "convexity" assumption of the energy functional)

However, the check of sequential lower semicontinuity might be hard in special cases. The need to relax the "convexity" assumption is that for finite elasticity, the uniqueness of the functionals minimizer is not fulfilled.

In [20] conditions are identified in order to establish that solutions of the incremental version (12) satisfy the time-continuous formulation (10) and (11). Additionally, a priori estimates for the solutions are found.

3. ADAPTION TO CFC

In order to adapt this framework to the situation of CFC, we have to specify several aspects: the relevant length scale as well as the fiber architecture (fiber bundles, fiber felts, etc.), the phases to be considered, the different contributions in the stored energy as well as the dissipation distance. All this is done in the following sections extending the first works in this direction [21]. We propose an elastic energy density as well as an interface energy for the case of CFC based on available experimental evidence (e.g., on the structure of the interfaces observed).

3.1. Choice of the Scale and Fiber Architecture

As already mentioned in the introduction, CFC is a typical multi-scale material. The energetic model developed here restricts itself first of all to one special length scale. Based on the energetic model on the scale chosen, appropriate methods have to be used in order to finally bridge the necessary scales and end up with a model for the macroscopic response for CFC.

Since CFC is not only multi-scale (Figure 3) but additionally shows a rich microstructure, we motivate our investigations by considering unidirectional carbon fiber bundles that have been infiltrated using the CVI process. Typically the carbon fibers have diameters of a few micrometers. On macroscopic scale, the structure of such CFC is schematically represented in Figure 3, left. We restrict ourselves then to the microscale and choose one single fiber including the deposited matrix of pyrolytic carbon around (Figure 3, right) as representative substructure in order to define the domain Ω under consideration.

3.2. Choice of the Phases

According to the scheme of classification of the microstructure of CFC [8], we define the set of phases to be

$$\mathcal{P} = \{LT, MT, HT\}. \qquad (13)$$

Though an isotropic phase is also known, we neglect this one based on experimental indications. Then, for $p \in \mathcal{P}$, the

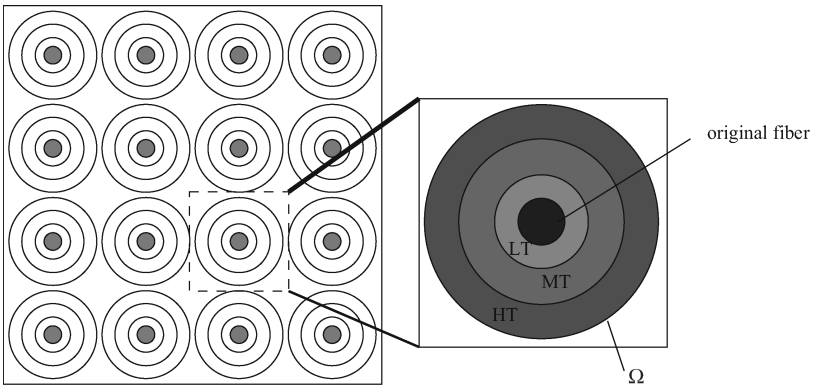

FIG. 3. Fiber bundle and domain of single fiber.

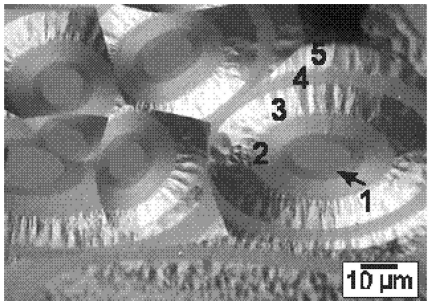

FIG. 4. Regions of different textures within CFC [6].

appropriate subdomain Ω_p where the internal state of the material belongs to phase p, is defined to be

$$\Omega_p = \{\boldsymbol{x} \in \Omega : \boldsymbol{s}(\boldsymbol{x}) = p\} \qquad \forall p \in \mathcal{P} \tag{14}$$

From the sharp interface structure, we directly find for $p_1, p_2 \in \mathcal{P}$

$$\Omega_{p_1} \cap \Omega_{p_2} = \emptyset \iff p_1 \neq p_2 \tag{15}$$

3.3. Choice of Energy Density

Despite that especially under high-temperature treatment, solid-solid-phase transitions between these three phases may occur, they all have to be regarded as stable phases.

Consequently a three-well contribution W_{3w} to the elastic energy density is assumed. The experimental evidence for solid-solid phase transformations especially under high temperature loading motivates us to assume that the local minima themselves depend on temperature:

$$W_{3\mathrm{w}}(\boldsymbol{x}, \boldsymbol{s}, \boldsymbol{Du}, \theta) = \left\| \boldsymbol{Du} - \sum_{p' \in \mathcal{P}} \mathbf{1}_{\Omega_{p'}}(\boldsymbol{x}) \boldsymbol{\xi}^{p'}(\theta) \right\|_{L^p}^m \tag{16}$$

with $m \geq 1$.

Additionally, the elastic energy density contains a contribution of the strain energy density. Here, we use thermoelasticity as a framework assuming different elasticity tensors $\mathcal{C}^{(p)}(\theta)$ for the different phases $p \in \mathcal{P}$, all of which are temperature dependent:

$$W_{strain}(\boldsymbol{x}, \boldsymbol{Du}(\boldsymbol{x}), \boldsymbol{s}(\boldsymbol{x}), \theta) = \sum_{p \in \mathcal{P}} 1_{\Omega_p}(\boldsymbol{x}) (\boldsymbol{Du} - \boldsymbol{\epsilon}^{th} - \boldsymbol{\xi}^{(p)}(\theta))_{ij} \mathcal{C}^{(p)}_{ijkl}(\theta) \left(\boldsymbol{Du} - \boldsymbol{\epsilon}^{th} - \boldsymbol{\xi}^{(p)}(\theta)\right)_{kl} \tag{17}$$

As described in the following subsection, this expression is based on sharp interfaces between pure phases of the material, i.e., no phase mixtures.

The thermal part of the energy density can be specified. Regarding the anisotropic behavior of the phases we define

$$W_{th}(\boldsymbol{x}, \boldsymbol{Du}(\boldsymbol{x}), \boldsymbol{s}(\boldsymbol{x}), \theta) = \int_{\theta_0}^{\theta} \sum_{p' \in \mathcal{P}} \mathbf{1}_{\Omega_{p'}}(\boldsymbol{x}) c^{(p')}(\theta') \mathrm{d}\theta' + \sum_{p' \in \mathcal{P}} \mathbf{1}_{\Omega_{p'}} b_{ij}^{(p')} (\boldsymbol{Du})_{ij} (\theta - \theta_0) \tag{18}$$

with the specific heat for each phase, $c^{(p')}(\theta)$, a symmetric tensor of second rank, $\boldsymbol{b}^{(p')}$, and with θ_0 as a reference temperature. Note that in the case of isotropy of phase p', we have $b_{ij}^{(p')} \propto \alpha \delta_{ij}$ with α as coefficient of linear thermal expansion.

The total free energy density is then given by the sum of the three-well contribution according to Eq. (16) and the part of the strain energy density Eq. (17):

$$W(\boldsymbol{x}, \boldsymbol{Du}(\boldsymbol{x}), \boldsymbol{s}(\boldsymbol{x}), \theta) = W_{3w} + W_{strain} + W_{th} \tag{19}$$

where the dependencies have been skipped to simplify the notation and can be found in Eqs. (16), (17) and (18).

3.4. Choice of Interface Energy

The expression for the interface energy directly determines the structure of the interfaces. If no interface energy is assumed, we obtain phase mixtures [18]. However, this is not the case for CFC (see Figures 1b and 4). If the interface energy is assumed to depend on the jumps of the internal states, sharp interfaces are obtained. Using higher gradients of the internal states, smooth interfaces can be obtained.

In a first assumption, we treat the interface energy as dependent on the surface tension σ and the 2D-Hausdorff measures of the boundaries $\mathcal{B}$. The surface tension itself is assumed to be constant, depending on the temperature θ and the adjacent phases, denoted by $\boldsymbol{s}_+$ and $\boldsymbol{s}_-$:

$$\mathcal{E}_{inter}(t, \boldsymbol{u}, \boldsymbol{s}, \theta) = \int_{\mathcal{B}} \sigma(\boldsymbol{s}_+, \boldsymbol{s}_-, \theta) \, \mathrm{d}\mathcal{H}^2 \tag{20}$$

3.5. About the Dissipation Distance

Within the framework of standard generalized materials [22], the dissipation distance can be determined based on the principle of maximum dissipation [23]. Here, the internal states and the thermodynamically conjugated force as well as the temperature and the entropy enter the definition of the dissipation distance. Note, however, that the dissipation could be calculated only for a very few cases so far [23] and the case of thermoelasticity is not among them. In case of a microscopic energetic model for shape memory alloys [16] with internal states as elements of $\mathbb{R}^m$ the dissipation distance for internal states $z_0, z_1 \in \mathbb{R}^m$ is chosen to be

$$\mathcal{D}(z_0, z_1) = \int_{\Omega} |z_0 - z_1| \, \mathrm{d}x \tag{21}$$

3.6. Multi-Scale Aspects

Above, we developed a microscale energetic model for CFC. However, as has been indicated in the introduction, the material

itself is multi-scale and moreover, we intend to model the macroscopic response. Thus, we have to look at how to bridge the scale and to arrive at the macroscale having started at the microscale as above. One established method (see e.g. [24]) is to quasiconvexify the functionals of the energy as well as of the dissipation distance on microscale given in Eqs. (4) and (8) which relaxes the ill-posed formulation on macroscale. Alternatively, we could ask whether these functionals on the microscale Γ-converge [25] and what the possible limits $\mathcal{E}_{mac}$ and $\mathcal{D}_{mac}$ look like. Consequently restrictions arise on the functionals on the microscale themselves. In the recent work [17] conditions have been stated for the existence of solutions of the limit problem of a series of incremental formulations of evolutionary problems and about the convergence of solutions. Since isothermal conditions are used, these results cannot be directly applied to the case of thermoelasticity here.

4. SUMMARY AND CONCLUSIONS

For describing the macroscopic response of CFC including phase transformations, the framework of rate-independent energetic models has been applied. To adapt this framework to the case of CFC means to fix the set of phases, the length scale and the domain. We have concentrated on unidirectional fiber bundles and consequently on microscale energetic models for non-isothermal situations for a domain consisting of a single fiber and the concentrically deposited matrix with three phases of pyrolytic carbon. Proposals for the interface energy and restrictions on the elastic energy density are derived. The conditions for existence of solutions of the defined extension of the energetic model to the non-isothermal situation remain to be investigated as well as properties of the solution. Expressions for the dissipation distances as well as for the temperature dependence are actually studied.

Finally, restrictions on the energy density will be obtained due to the existence and uniqueness theorems in the framework of Γ-convergence for the description of the macroscopic material properties.

ACKNOWLEDGEMENTS

The authors gratefully acknowledge partial funding by the Deutsche Forschungsgemeinschaft within the Centre of Excellence "Carbon from the gas phase: elementary reactions, structures, materials."

REFERENCES

1. Stadler, Z., Krnel, K., and Kosmac, T., "Friction behavior of sintered metallic brake pads on a C/C-SiC composite brake disc," *Journal of the European Ceramic Society* **27**, 1411–1418 (2007).
2. Kaneda, H., Onaka, T., Nakagawa, T., Enya, K., Murakami, H. et al., "Cryogenic optical performance of the ASTRO-F SiC telescope," *Applied Optics* **44**, 6823–6832 (2005).
3. Zhou, Y., and Xia, Y., "Experimental study of the rate-sensitivity of unidirectional-fiber-reinforced metal-matrix composite wires and the establishment of a dynamic constitutive equation," *Composites Science and Technology* **61**, 2025–2032 (2001).
4. Langhoff, T.-A., and Schnack, E., "Modelling chemical vapour infiltration of pyrolytic carbon," in W. Wendland, M. Effendiev (eds). *Lecture Notes in Applied and Computational Mechanics* **12**, 149–154, Springer, (2003).
5. De Pauw, V., Reznik, B., Kalhöfer, S., Gerthsen, D., Hu Z. J., and Hüttinger, K. J., "Texture and nanostructure of pyrocarbon layers deposited on planar substrates in a hot-wall reactor," *Carbon* **41**, 71–77 (2003).
6. Reznik, B., and Gerthsen, D., "Microscopic study of failure mechanisms in infiltrated carbon fibre felts," *Carbon* **41**, 57–69 (2003).
7. Guellali, M., Oberacker, R., and Hoffmann, M. J., "Influence of the matrix microstructure on the mechanical properties of CVI-infiltrated carbon fiber felts," *Carbon* **43**, 1954–1960 (2005).
8. Reznik, B., and Hüttinger, K.-J., "On the terminology for pyrolytic carbon," *Carbon* **40**, 621–623 (2002).
9. Bourrat, X., Trouvat, B., Limousin, G., and Vignoles, G., "Pyrocarbon anisotropy as measured by electron diffraction and polarize light," *J. Mater. Res.* **5**, 92–101 (2000).
10. Delhaes, P., "Attempts to chemical vapour infiltrate pyrocarbons: evidence for a spatial bistability?" *Carbon* **41**, 1093–1095 (2003).
11. Delhaes, P.,"Chemical vapor deposition and infiltration processes of carbon materials," *Cabon* **40**, 641–657 (2002).
12. Loll, P., Delhaes, P., Pacault A. and Pierre A., "Diagramme d'existence et proprietes de composites carbone-carbone," *Carbon* **15**, 383–390 (1977).
13. Guellali, M., Oberacker, R., and Hoffmann, M. J., "Influence of heat treatment on microstructure and mechanical properties of CVI-infiltrated carbon fibre felts with medium and highly textured pyrocarbon matrices," Proceedings of International Carbon Conference, Gyeongju, Korea, July 3–7 (2005).
14. Piat, R., and Schnack, E., "Hierarchical material modeling of carbon/carbon composites," *Carbon* **41**, 2121–2129 (2003).
15. Bartels, S., Carstensen, C., Hackl, K., and Hoppe, U., "Effective Relaxation for Microstructure Simulations: Algorithms and Applications," *Comput. Methods Appl. Mech. Engrg.* **193**, 5143–5175 (2004).
16. Mainik, A., and Mielke, A., "Existence results for energetic models for rate-independent systems," *Calc. Var. PDEs* **22**, 73–99 (2005).
17. Mielke, A., A model for temperature-induced phase transformation in finite-strain elasticity, *IMA J. Applied Math* **72**(5), 644–658 (2007).
18. Mielke, A., Theil, F., and Levitas, V. I., "A Variational Formulation of Rate-Independent Phase Transformations Using an Extremum Principle," *Arch. Rational Mech. Anal.* **162**, 137–177 (2002).
19. Mielke, A., and Theil, F., "On rate-independent hysteresis models," *Nonl. Diff. Eqns. Appl (NoDEA)* **11**, 151–189 (2004).
20. Francfort, G., and Mielke, A., "Existence results for a class of rate-independent material models with nonconvex elastic energies," *J. Reine Angew. Math.* **595**, 55–91 (2006).
21. Langhoff, T.-A., and Schnack, E., "Energetic modelling for carbon fibre reinforced carbon," *PAMM* **6**, 495–496 (2006).
22. Hackl, K., "Generalized standard media and variational principles in classical and finite strain elastoplasticity," *J. Mech. Phys. Solids* **45**, 667–688 (1997).
23. Mielke, A. "Energetic formulation of multiplicative elasto-plasticity using dissipation distances," *Continuum Mech. Thermodyn.* **15**, 331–382 (2003).
24. Miehe, C., and Lambrecht, M., "A two-scale finite element relaxation analysis of shear bands in non-convex inelastic solids: small-strain theory for standard dissipative materials," *Computer Meth. in Appl. Mech. Engnrg.* **192**, 473–508 (2003).
25. DalMaso, G., An introduction to Gamma-Convergence, Birkhäuser, Basel 1993.
26. Mielke, A., Roubicek, T., and Stefanelli, U., Γ-limits and relaxations for rate-independent evolutionary problems, *Calc. Var. Part. Diff. Equ.* **31**, 387–416 (2008).